

BagChain: A Dual-functional Blockchain Leveraging Bagging-based Distributed Learning

Zixiang Cui, Xintong Ling, *Member, IEEE*, Xingyu Zhou, Jiaheng Wang, *Senior Member, IEEE*,
Zhi Ding, *Fellow, IEEE*, Xiqi Gao, *Fellow, IEEE*

Abstract—This work proposes a dual-functional blockchain framework named BagChain for bagging-based decentralized learning. BagChain integrates blockchain with distributed machine learning by replacing the computationally costly hash operations in proof-of-work with machine-learning model training. BagChain utilizes individual miners' private data samples and limited computing resources to train base models, which may be very weak, and further aggregates them into strong ensemble models. Specifically, we design a three-layer blockchain structure associated with the corresponding generation and validation mechanisms to enable distributed machine learning among uncoordinated miners in a permissionless and open setting. To reduce computational waste due to blockchain forking, we further propose the cross fork sharing mechanism for practical networks with lengthy delays. Extensive experiments illustrate the superiority and efficacy of BagChain when handling various machine learning tasks on both independently and identically distributed (IID) and non-IID datasets. BagChain remains robust and effective even when facing resource-constrained mobile devices, heterogeneous private user data, and sparse wireless network connectivity.

Index Terms—Bagging, blockchain, consensus protocol, distributed learning, proof-of-useful-work.

I. INTRODUCTION

The proliferation of mobile devices that collect data with powerful sensors like cameras and microphones enables the possibility of constructing more powerful intelligent applications. However, the centralized machine learning (ML) approach is facing certain challenges in exploiting private data and computing power on mobile devices. First of all, data transmissions from users to data centers over bandwidth-limited networks are time-consuming and costly. Second, users are also unwilling to share their sensitive information with data centers, precluding them from harnessing such data for ML purposes. Third, users' private data may be non-independently and identically distributed (non-IID), which significantly increases the bias of the ML models trained with mobile devices' private data [1]. Last but not least, mobile devices lack the computing capability required to train high-quality ML models.

Zixiang Cui, Xintong Ling, Xingyu Zhou, Jiaheng Wang, and Xiqi Gao are with the National Mobile Communications Research Laboratory, Southeast University, Nanjing 210096, China (email: zxcui@seu.edu.cn; xtling@seu.edu.cn; zhouxingyu319@gmail.com, jhwang@seu.edu.cn; xqgao@seu.edu.cn). Xintong Ling, Jiaheng Wang, and Xiqi Gao are also with the Purple Mountain Laboratories, Nanjing 210023, China.

Zhi Ding is with the Department of Electrical and Computer Engineering, University of California at Davis, Davis, CA 95616 USA (e-mail: zding@ucdavis.edu).

Some distributed learning techniques like federated learning (FL) [2] and consensus learning (CL) [3] can harness computing resources and heterogeneous private data on mobile devices to train ML models. In FL systems, data holders train local models with their private data, and the local models are then uploaded and aggregated into a global model by a central server. CL is a fully decentralized approach where each node updates the local model by aggregating the model parameters received from the neighboring nodes in a mesh network.

However, cooperative ML for on-device distributed learning faces several challenges when migrating existing distributed learning approaches to peer-to-peer open networks, which may include untrustworthy or faulty nodes. In some distributed learning techniques like FL, centralized network topology incurs single-point-of-failure vulnerability and communication bottlenecks at the central server [4]. The iterative training procedures in FL also incur huge communication overhead, which is unbearable for both mobile devices and central servers. Other techniques like CL assume a fixed network topology, which is not feasible in dynamic network environments allowing nodes to join or leave frequently. Currently, most distributed learning techniques are set up in trustworthy closed systems where data access and contributions from external nodes are prohibited, while the open and untrustworthy environment may pose security risks like poisoning attacks to these methods.

Blockchain is a game-changing innovation that subverts the conventional centralized paradigm and has shown its potential for various applications [5]–[7]. It exploits consensus protocols and cryptographic tools to store data consistently and immutably in an open and untrustworthy network. Compared with centralized solutions, blockchain is more scalable and resilient to single-point failures and malicious entities.

Serving as a decentralized foundation, blockchain is capable of offering promising solutions to the challenges in existing distributed learning techniques. Each node executes consensus protocols and validates on-chain data independently to mitigate the risk of malfunctioning or dishonest nodes compared with centralized ML systems. With the help of blockchain, ML systems are more friendly to external participants than conventional ML systems because participants can join the distributed learning process freely without being permitted or managed by any central node. Moreover, blockchain can incentivize participants to contribute their computing power and private data for distributed ML model training.

A. Related Work

Since 2019, numerous studies have adapted blockchain systems to various ML tasks such as biomedical image segmentation model training [8], cloud-edge-end resource allocation [9], neural architecture searching [10], and medical image fusion [11] to leverage computing power and data in a blockchain network. Several studies [12]–[17] utilized blockchain as an ML competition platform, where ML model training, evaluation, and ranking procedures are embedded in the workflow of the blockchain system. In such systems, model checkers filter out unqualified model parameters or updates based on performance evaluation on a test dataset provided by the model requester, and the node that trains the best ML model within the least time sends its model to the model requester and receives the training reward. However, the above approaches, which select and reward only one single winning model from several models trained on specific datasets and discard the rest, fail to take full advantage of miners’ computing power and private data samples.

As a collaborative ML approach that can harness device-side private data in a privacy-preserving manner, FL can be blended with blockchain systems better than the aforementioned blockchain-based ML competition schemes. Several studies implemented FL algorithms in blockchain systems via smart contracts [18], [19]. A more fundamental approach is integrating FL with customized consensus protocols so that the FL system can become self-incentivized and more robust to malicious behaviors. For instance, in proof-of-federated-learning (PoFL) [20], Qu *et al.* adapted the mining pools in proof-of-work (PoW) blockchain into federations of miners, where the miners in a mining pool collaboratively train a global model with algorithms like federated averaging and the pool manager broadcasts the block containing the global model. In [21], the authors eliminated the trusted third-party platform in PoFL with a new block structure, extra transaction types, and a credit-based incentive mechanism. In FedCoin [22], a Shapley-value-based consensus protocol, the quality of local models was considered before allocating training rewards by evaluating the contribution of each miner’s local model to the global model. In [23], [24], the authors combined directed acyclic graph (DAG) blockchain with FL to avoid the drain of computing resources in PoW systems and protect FL from lazy nodes and poisoning attacks. However, in many blockchain-based FL systems, the FL iterations are administered by a few centralized servers (e.g., the mining pool managers in PoFL) or third-party platforms, which compromises the degree of decentralization of the entire system. Though this issue has been considered in the above two works using DAG-based asynchronous FL, the low utilization of local models affects the convergence rate of the global model and degrades the learning performance [25].

Highlight that ML can serve as useful work in proof-of-useful-work (PoUW) as an alternative to PoW and improves the environmental sustainability of conventional PoW systems by replacing the computing power consumed in meaningless hash calculations with some useful computation tasks like ML model training. Most ML-based PoUW protocols like proof-of-deep-learning (PoDL) [13], personalized artificial intelligence [26], proof-of-learning (PoL) [27], RPoL [26], and

distributed PoDL [28] use the same principle where miners attest certain amounts of honest computation by providing the intermediate parameters necessary for reproducing the final ML model. Such protocols involve intense communication and computation overhead because ML model retraining or verifying intermediate training steps are necessary when validating miners’ workloads. To avoid transmitting all the intermediate model parameters directly, in DLchain [29], miners execute training algorithms like stochastic gradient descent with fixed random seeds and prove training work with the random seeds and the accuracies of the model at each epoch. Also, zero-knowledge PoL [30] significantly reduced the communication, computation, and storage overhead for Internet of Things devices via zero-knowledge proof techniques. Nevertheless, even so, the computational amount involved in PoUW proof generation or validation remains unacceptable for resource-constrained mobile devices.

B. Our Contributions

In our work, we propose BagChain by integrating the blockchain protocol with bagging, an ensemble learning algorithm [31]. BagChain serves as a dual-functional blockchain framework targeting two purposes together: distributed machine learning and blockchain consensus maintenance. Specifically, we design the three-layer blockchain structure for BagChain and utilize the computational power for useful ML model training instead of meaningless hash operations in PoW. It features a fully decentralized architecture without relying on central nodes or trusted third parties. In BagChain, all miners train the possibly weak base models by using their local computing power and private data and aggregate the base models into an ensemble model, which exhibits satisfactory performance according to the experimental results in Section VII. Notably, these base models are trained on miners’ private datasets, obviating the need to reveal or share raw data, and BagChain can tolerate these private datasets being imbalanced or non-IID. Furthermore, each base model could be very weak since it requires only a short training period of 10 to 20 epochs, and thus BagChain is feasible even for resource-constrained mobile nodes. Furthermore, since the bagging algorithm only requires one-time prediction-level aggregation rather than the iterative global model aggregation in FL, BagChain has a lower communication overhead than vanilla FL and is thus suitable for bandwidth-limited wireless networks. We have released the code of BagChain at: <https://github.com/czxdev/BagChain>.

The main contributions of our work are summarized below:

- We propose BagChain, a dual-functional blockchain framework that enables generic ML task execution and integration of the bagging algorithm in a public blockchain network. To the best of our knowledge, it is the first work integrating blockchain into bagging-based distributed learning algorithms.
- We propose the three-layer blockchain structure of BagChain with block generation and validation algorithms to enable the automation of model training,

aggregation, and evaluation in a fully decentralized setting.

- We introduce a cross fork sharing mechanism to reduce computing power waste resulting from blockchain forking. The mechanism maximizes the utilization of the base models and improves the performance of the ensemble models by including the hash values of as many MiniBlocks in Ensemble Blocks as possible.
- We discuss the performance issues and security implications of BagChain including model plagiarism and blockchain forking, and design a task queuing mechanism to improve BagChain's resilience to blockchain forking.
- We conduct ChainXim-based simulations for BagChain on the commonly used image classification tasks to demonstrate the benefits of exploiting non-IID private data and pooling computing power simultaneously and to validate the feasibility of BagChain under different network conditions.

The remaining part of the paper is organized as follows. In Section II, we present the system model. We show the framework of BagChain and the validation procedures in Section III and Section IV, respectively. We design the cross fork sharing mechanism in Section V. In Section VI, we discuss the security and performance. In Section VII, we provide the results of ChainXim-based experiments to demonstrate the efficacy of BagChain. Section VIII draws a conclusion.

II. SYSTEM MODEL

A. Distributed Learning Scenario

In this work, we consider a distributed learning scenario where some requester nodes have demands for ML-based intelligent applications and can offer financial incentives in exchange for ML model training services. Meanwhile, some nodes, referred to as miners, are willing to contribute their private data and computing power to ML tasks published by these requesters. However, miners are unwilling to share their private data due to privacy concerns and might have difficulty training high-quality ML models independently since they may be mobile devices with limited capabilities. Besides executing ML tasks, these miners also need to maintain the blockchain network by generating new blocks.

In the considered scenario, we assume the label or feature distributions across different miners' private datasets can be heterogeneous. Meanwhile, we assume all requesters follow the rules of our framework, e.g., publishing sound tasks and releasing datasets in time, because they have paid training fees when publishing ML tasks and lack the motivation to disrupt the ML training process.

B. Supervised Learning Model

In our work, every ML task employs a supervised learning approach where ML models can be described by parameterized functions $f(\cdot; \omega)$ trained on a dataset D . Each ML model can make predictions with the input features and is uniquely determined by the model framework f and the model parameters ω . Each dataset D is composed of a feature matrix

and a label vector (\mathbf{X}, \mathbf{y}) . Each row of \mathbf{X} denotes the feature vector of a sample, and the corresponding \mathbf{y} represents the categorical label of the sample for classification tasks. Four datasets are involved: public training dataset $D_T = (\mathbf{X}_T, \mathbf{y}_T)$, private dataset $D_{M_i} = (\mathbf{X}_{M_i}, \mathbf{y}_{M_i})$ that miner M_i possesses, validation dataset $D_V = (\mathbf{X}_V, \mathbf{y}_V)$, and test dataset $D_E = (\mathbf{X}_E, \mathbf{y}_E)$. The public training dataset D_T is available to all the miners and is published by the requester before ML task execution. Meanwhile, every miner's private dataset may be non-IID and heterogeneous. Mathematically, $|D|$ means the number of samples in the dataset D , and $D_1 \cup D_2$ represents the union of D_1 and D_2 . We focus on the learning process and omit data standardization and the other pre-processing steps.

The bagging algorithm involves four operations. The operation $\text{Train}(\cdot; f)$, parameterized by the model framework f , takes any dataset D as input and outputs the model parameters ω trained on D . The operation $\text{Resample}(\cdot)$ performs random sampling with replacement on the input dataset. The operation $\text{Aggregate}(\cdot)$ takes the output values of a sequence of base models as input and outputs the final predictions of the ensemble of the base models using a specific aggregation rule, typically a majority vote for classification tasks. The operation $\text{Metric}(\cdot, \cdot)$ takes the predicted labels and the correct labels as inputs and outputs the performance metric that evaluates the discrepancies between the two input vectors. The metric can be accuracy, recall, precision, or F1-score for classification tasks.

C. Blockchain Model

We consider a permissionless blockchain where any individual can participate in the maintenance of the blockchain network, and on-chain data are accessible to all participants. The blockchain network is an open peer-to-peer network of numerous miners, who execute ML tasks and propose new blocks to win rewards. We denote the blockchain network with N miners as $\mathcal{M} = \{M_1, M_2, \dots, M_N\}$, in which each element is the identifier (ID) of a miner.

Blockchain C is a chain of one-way linked blocks containing payload data like transactions and smart contracts. A block is denoted as B_h , where h means block height, the number of blocks counted from the genesis block B_0 to B_h . The timestamp included in every block B_i is denoted as $T(B_i)$. We represent C with a sequence of blocks as: $C = \{B_0 \rightarrow B_1 \rightarrow \dots \rightarrow B_h\}$, where the subscript h is the block height of B_h , i.e., the length of C . Each miner M_i in the blockchain network \mathcal{M} maintains its local replica of the blockchain, which is the local chain of M_i and denoted as C_i . The predefined rule that the miners comply with to append new blocks to the chain is called a consensus protocol. Typically, a consensus mechanism is composed of two major operations: block generation and block validation. The latter operation takes a block as input and is denoted as $\text{Validate}(\cdot)$.

In practice, network delay might incur race conditions where new blocks fail to reach all the nodes in the network in time before another block is generated. From a global perspective, the race conditions cause asynchronous states in the blockchain network, resulting in extra branches diverging from the main chain, i.e., forks [32]. We denote the block on

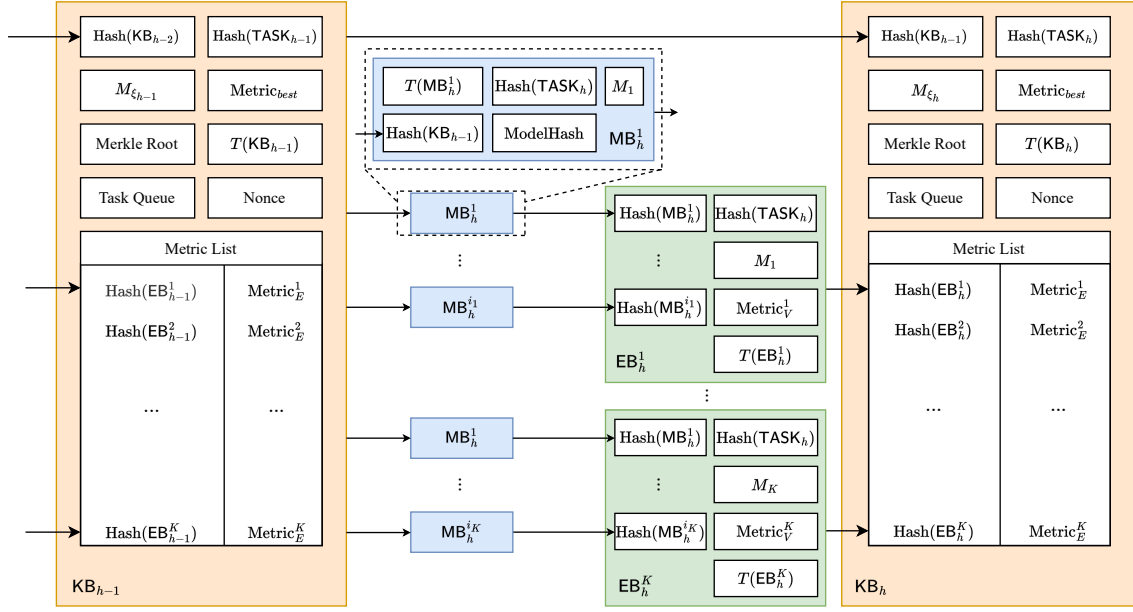


Fig. 1. Overview of the proposed three-layer blockchain structure.

the main chain C at block height k as B_k and the fork at block height $k + 1$ as \tilde{B}_{k+1} , which links to the same block B_k as B_{k+1} . We assume every miner only has a local view of the blockchain and extends the local chain according to the consensus protocol.

Cryptographic hash functions are extensively utilized in blockchain systems to eliminate block tampering and Sybil attacks. They are usually modeled as random oracles, which output a fixed-length value for every unique input of arbitrary length, and are denoted as $\text{Hash}(\cdot)$ in this paper. The input of $\text{Hash}(\cdot)$ might be any data object or the concatenation of multiple objects, symbolized by \parallel between objects. Also, the hash value of the preceding block that B points to is called the prehash of B .

D. Network Model

We describe peer-to-peer networks with two operations: $\text{Broadcast}_{\mathcal{M}}(\cdot)$ and $\text{Fetch}(\cdot, \cdot)$. The operation $\text{Broadcast}_{\mathcal{M}}(\cdot)$ propagates messages such as blocks and payload data across the entire blockchain network \mathcal{M} so that all the miners can receive the message. The operation $\text{Broadcast}_{\mathcal{M}}(\cdot)$ varies with different network models. For example, in a fully-connected network, when a node generates a new block B and diffuses it to the rest of the network \mathcal{M} via $\text{Broadcast}_{\mathcal{M}}(B)$, the other nodes in the network \mathcal{M} will receive the newly generated block B after a given constant delay. We also consider the mesh network model, a harsher network model with sparse connections, to simulate wireless scenarios. In the mesh network model, the transmission delay of a data object between two nodes in the network is directly proportional to the object size and inversely proportional to the link bandwidth between the two nodes.

The operation $\text{Fetch}(\cdot, \cdot)$ is for the point-to-point transmission of model parameters or datasets. When node M_j invokes $\text{Fetch}(M_i, \text{Hash}(\Theta))$, it sends a query to node M_i with the identifier $\text{Hash}(\Theta)$ and downloads the

data object Θ . We assume the mining network can support downloading models and datasets within an acceptable delay through $\text{Fetch}(\cdot, \cdot)$.

III. FRAMEWORK OF BAGCHAIN

A. Blockchain Structure

In this section, we show the proposed BagChain framework and how BagChain realizes bagging-based distributed learning via a blockchain approach. First, we design the blockchain structure of BagChain. To enable requesters to publish ML tasks and disclose validation and test datasets, the data structure of ML tasks is defined as a seven-element tuple: $\text{TASK} = (\text{Hash}(D_T), \text{Hash}(D_V), \text{Hash}(D_E), \text{Train}(\cdot; f), \text{Aggregate}(\cdot), \text{Metric}(\cdot, \cdot), \text{Metric}_{\min})$. The fourth to sixth items correspond to the script used for model training, aggregation, and evaluation. The parameter f in $\text{Train}(\cdot; f)$ and the minimum requirement Metric_{\min} for ML model performance metrics are specified by the requester. Any requester can publish TASK via a task publication transaction, which further includes the model training fees, and the requester's digital signature and ID. The ML task to be executed at block height h is denoted as TASK_h . A requester can publish the validation or test dataset via the dataset publication message, which consists of the current block height h , the type of the published dataset, the timestamp of the publishing moment when the validation or test dataset is published, the ongoing task ID $\text{Hash}(\text{TASK}_h)$, and the requester's digital signature.

Specifically, to integrate with the distributed bagging algorithm, we design a three-layer blockchain structure consisting of MiniBlocks, Ensemble Blocks, and Key Blocks. The structures and interconnections of MiniBlocks, Ensemble Blocks, and Key Blocks are depicted in Fig. 1.

- *MiniBlock* (MB_h^i) contains a unique base model and records the ownership of the base model and the hash identifier of its parameters $\text{ModelHash} = \text{Hash}(\omega_i \parallel M_i)$.

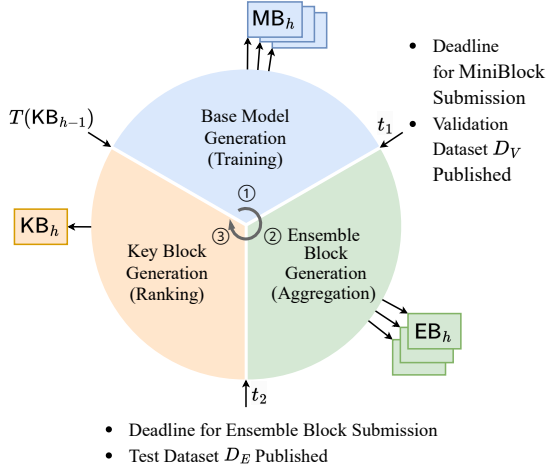


Fig. 2. Workflow of BagChain and lifecycle of a learning task.

- *Ensemble Block* (EB_h^k) points to several MiniBlocks to form an ensemble model and also includes the ensemble model's metric $Metric_V^k$ on the validation dataset D_V .
- *Key Block* (KB_h) includes the ensemble model rank, task queue, and also blockchain payload data. In KB_h , M_{ξ_h} , $Metric_E^j$, and $Metric_{best}$ represent the ID of the producer of KB_h , the metric of EB_h^j on the test dataset D_E , and the metric of the best ensemble model, respectively.

B. Workflow

The workflow of BagChain enables fully decentralized coordination of miners and requesters. It includes three phases, as illustrated in Fig. 2. We assume the corresponding task publication transaction has already been broadcast, validated by miners, and recorded on the blockchain.

Phase I: Base model training. The generation and propagation of a new Key Block KB_{h-1} trigger the first phase of the execution of a new task, denoted as $TASK_h$. If miner M_i receives multiple valid chains of different lengths, it will extend the longest chain; otherwise, miner M_i will extend the chain with optimal $Metric_{best}$. Once miner M_i confirms KB_{h-1} , miner M_i will execute Algorithm 1.1 to train a base model and generate a MiniBlock. Miner M_i first initiates the executable scripts and prepares the local training dataset D_{T_i} , which includes its private dataset D_{M_i} and the public training dataset D_T . Then, miner M_i executes the training script on the bootstrapped local dataset D_{T_i} and generates the parameters of a base model, denoted as $\omega_i = \text{Train}(\text{Resample}(D_{T_i}); f)$. Once the base model is ready, miner M_i encapsulates a timestamp $T(MB_h^i)$, miner's ID M_i , $\text{Hash}(TASK_h)$, ModelHash , and $\text{Hash}(KB_{h-1})$ into MB_h^i and diffuses the MiniBlock via $\text{Broadcast}_{\mathcal{M}}(MB_h^i)$. All the miners should keep their base models secret in Phase I to avoid plagiarism.

Phase II: Ensemble Block Generation. Phase II starts at a pre-determined time t_1 . At t_1 , the requester discloses the validation dataset D_V via a validation dataset publication message. Once the validation dataset D_V is released, any MiniBlock afterward should be rejected since they may be trained by overfitting the validation data. An honest miner M_i will generate a new Ensemble Block according to Algorithm

Algorithm 1.1 MiniBlock Generation

Input: KB_{h-1}, M_i, D_{M_i}

Output: MB_h^i

- 1: $TASK_h \leftarrow KB_{h-1}$
- 2: $f, \text{Train}(\cdot), \text{Hash}(D_T) \leftarrow TASK_h$
- 3: $D_T \leftarrow \text{Fetch}(\text{requester}, \text{Hash}(D_T))$
- 4: $D_{T_i} \leftarrow D_T \cup D_{M_i}$
- 5: $\omega_i \leftarrow \text{Train}(\text{Resample}(D_{T_i}); f)$
- 6: $MB_h^i \leftarrow \{T(MB_h^i) || \text{Hash}(TASK_h) || \text{ModelHash} || M_i || \text{Hash}(KB_{h-1})\}$

Algorithm 1.2 Ensemble Block Generation

Input: $MB_h^1, \dots, MB_h^{\hat{J}}, M_i, KB_{h-1}$

Output: EB_h^i

- 1: $TASK_h \leftarrow KB_{h-1}$
- 2: $\text{Aggregate}(\cdot) \leftarrow TASK_h$
- 3: **for** $j \leftarrow 1$ to \hat{J} **do**
- 4: **if** $\text{Validate}(MB_h^j) = \text{False}$ **or** prehash of $MB_h^j \neq \text{Hash}(KB_{h-1})$ **then**
- 5: Discard MB_h^j
- 6: **end if**
- 7: **end for** ▷ J out of \hat{J} MiniBlocks are valid
- 8: $Metric_V^i \leftarrow \text{Metric}(\text{Aggregate}(f(\mathbf{X}_V; \omega_1), \dots, f(\mathbf{X}_V; \omega_J)), \mathbf{y}_V)$
- 9: $EB_h^i \leftarrow \{\text{Hash}(MB_h^1) || \dots || \text{Hash}(MB_h^{\hat{J}}) || \text{Metric}_V^i || M_i || \text{Hash}(TASK_h) || T(EB_h^i)\}$

1.2, which can be summarized into four steps. a) Download the validation dataset D_V and execute $\text{Fetch}(M_j, \text{ModelHash})$ to fetch the parameters ω_j , in which ModelHash is extracted from MB_h^j . b) Execute $\text{Validate}(MB_h^j)$ for all the MiniBlocks that are collected by miner M_i and point to KB_{h-1} on the top of miner M_i 's local chain C_i . The MiniBlocks that are invalid or point to the Key Blocks other than KB_{h-1} are discarded. c) Evaluate the ensemble of all the available base models with the validation dataset D_V by calculating $Metric_V^i = \text{Metric}(\text{Aggregate}(f(\mathbf{X}_V; \omega_1), \dots, f(\mathbf{X}_V; \omega_J)), \mathbf{y}_V)$, where J is the total number of the valid MiniBlocks collected by miner M_i . d) Encapsulate a timestamp $T(EB_h^i)$, miner's ID M_i , $\text{Hash}(TASK_h)$, $Metric_V^i$, and $\text{Hash}(MB_h^j)$ into EB_h^i . The newly generated Ensemble Block EB_h^i is disseminated by executing $\text{Broadcast}_{\mathcal{M}}(EB_h^i)$. If miner M_i receives any Ensemble Block EB_h^q from other miners, miner M_i will verify EB_h^q with $\text{Validate}(EB_h^q)$ (see Algorithm 2.2) and further forward EB_h^q to neighboring miners.

Phase III: Key Block Generation. Similar to Phase II, Phase III starts at another pre-determined time t_2 . At t_2 , the requester discloses the test dataset D_E . Once miner M_i downloads the test dataset D_E , it verifies the Ensemble Blocks, denoted by EB_h^1, \dots, EB_h^K , and evaluates them on the test dataset D_E , and attempts to create a new Key Block via Algorithm 1.3. Then, miner M_i measures the performance of the Ensemble Blocks, e.g., EB_h^j , via $Metric_E^j = \text{Metric}(\text{Aggregate}(f(\mathbf{X}_E; \omega_{j,1}), \dots, f(\mathbf{X}_E; \omega_{j,\eta_j})), \mathbf{y}_E)$, where $\omega_{j,\ell}$ is the parameters of the base model ensemble in EB_h^j . Miner M_i ranks all the ensemble models from the

Algorithm 1.3 Key Block Generation

Input: $EB_h^1, \dots, EB_h^K, M_i, KB_{h-1}$
Output: KB_h

```

1:  $TASK_h \leftarrow KB_{h-1}$ 
2:  $Hash(D_E) \leftarrow TASK_h$ 
3:  $\mathbf{X}_E, \mathbf{y}_E \leftarrow D_E \leftarrow \text{Fetch}(\text{requester}, Hash(D_E))$ 
4: for  $j \leftarrow 1$  to  $K$  do
5:    $MB_h^1, \dots, MB_h^{\eta_j} \leftarrow EB_h^j$ 
6:   if  $\text{Validate}(EB_h^j) = \text{False}$  then
7:     Discard  $EB_h^j$ 
8:   end if
9:    $\text{Metric}_E^j \leftarrow \text{Metric}(\text{Aggregate}(f(\mathbf{X}_E; \omega_{j,1}), \dots, f(\mathbf{X}_E; \omega_{j,\eta_j})), \mathbf{y}_E)$ 
10: end for  $\triangleright K$  out of  $K$  Ensemble Blocks are valid
11:  $\text{Nonce} \leftarrow 0$ 
12:  $\text{Metric}_{best} \leftarrow \max(\text{Metric}_E^1, \dots, \text{Metric}_E^K)$ 
13: repeat
14:    $KB_h \leftarrow \{\text{Nonce} || \text{Merkle Root} || T(KB_h) || \text{Metric}_{best} || \text{Hash}(EB_h^1) || \text{Metric}_E^1 || \dots || \text{Hash}(EB_h^K) || \text{Metric}_E^K || M_i || \text{Hash}(TASK_h) || \text{Task Queue} || \text{Hash}(KB_{h-1})\}$ 
    $\triangleright \text{Metric}_E^1 \geq \text{Metric}_E^2 \geq \dots \geq \text{Metric}_E^K$ 
15:    $\text{Nonce} \leftarrow \text{Nonce} + 1$ 
16: until  $\text{Hash}(KB_h) < \text{Target}$ 
```

Ensemble Blocks EB_h^1, \dots, EB_h^K and finds the best model with the optimal Metric_E^q . At last, miner M_i deletes $TASK_h$ from the task queue and appends a new task to the tail of the task queue before it puts the necessary components of a Key Block into a candidate block \widehat{KB}_h . Miner M_i performs hash trials to find a suitable nonce satisfying $\text{Hash}(\widehat{KB}_h) < \text{Target}$ to generate a new Key Block \widehat{KB}_h and broadcast it to the rest of the network via $\text{Broadcast}_{\mathcal{M}}(\widehat{KB}_h)$. In our paper, Target is a threshold controlling the difficulty of generating Key Blocks, similar to PoW.

C. Incentive Mechanism

In BagChain, miners generating Key Blocks and MiniBlocks are rewarded because the miners generate valid MiniBlocks and Key Blocks to prove a certain amount of CPU or GPU resources has been consumed in ML model training and evaluation. Honest generators of Key Blocks conform to the following rules to allocate rewards. 1) The training fees from the requester are evenly distributed to all the miners producing the MiniBlocks that the winning Ensemble Block points to. 2) The Key Block reward is transferred to the generator of the Key Block. Since the selection of the winning Key Block is partly dependent on Metric_{best} , every miner will hunt for the best ensemble model by collecting as many Ensemble Blocks as possible in Phase III to obtain the Key Block reward. Though the miner generating the winning Ensemble Block will not be rewarded, the generators of MiniBlocks will be eager to generate Ensemble Blocks in Phase II since they must ensure the hash values of their MiniBlocks are included in at least one of the Ensemble Blocks to earn the training fees from the requester.

IV. BLOCK VALIDATION

BagChain's openness and permissionless setting lower the access barrier but lead to new challenges since the open environment is less trustworthy. The block generation rules in Section III-B can hardly be enforced on dishonest nodes or adversaries. For example, lazy nodes can compromise learning performance by plagiarizing other nodes' models, and malicious nodes can disrupt the distributed learning process. Consequently, BagChain requires efficient validation mechanisms that provide quality and integrity guarantees for the produced models.

In this section, we will show the validation procedures of MiniBlocks, Ensemble Blocks, and Key Blocks, respectively. Before validating any of the three blocks generated at block height h , we assume miner M_i has received $TASK_h$, and extracted f , $\text{Aggregate}(\cdot)$, $\text{Metric}(\cdot, \cdot)$, $\text{Hash}(D_V)$, and also $\text{Hash}(D_E)$ from $TASK_h$, and downloaded the corresponding validation or test datasets. Every miner maintains a local cache to store downloaded data objects. If the Ensemble Blocks, MiniBlocks, or model parameters ω_p involved in the validation procedures are not available in the local cache, miner M_i will execute $\text{Fetch}(\cdot, \cdot)$ to download the necessary data objects.

A. MiniBlock

After miner M_i receives a new MiniBlock MB_h^j , it verifies MB_h^j with $\text{Validate}(MB_h^j)$ shown in Algorithm 2.1 through the following steps:

- 1) Download the model parameters ω_j and verify whether $\text{Hash}(\omega_j || M_j)$ matches the hash value ModelHash in MB_h^j .
- 2) Check whether the corresponding $\text{Metric}(f(\mathbf{X}_V; \omega_j), \mathbf{y}_V)$ surpasses Metric_{min} of $TASK_h$, where $D_V = (\mathbf{X}_V, \mathbf{y}_V)$ is the validation dataset specified in $TASK_h$.

Our design aims to solidify the base models and their ownership in the MiniBlocks immutably and also to guarantee that the performance of the base models is acceptable. We meet requesters' performance requirements with step 2, where any base model with unacceptable performance on the newly released validation dataset D_V is invalidated. Also, we verify the integrity and ownership of the base model with step 1, where the non-invertible hash function $\text{Hash}(\cdot)$ can detect any error in model parameters ω_j or manipulation of miner ID M_j . We also prevent lazy miners from uploading other miners' base models to BagChain with a two-stage model submitting scheme, where new MiniBlocks and corresponding base models will be rejected by honest miners after the validation dataset is disclosed. From this point on, the base models that can be aggregated in Phase II are immutable.

B. Ensemble Block

After miner M_i receives a new Ensemble Block EB_h^q , it verifies EB_h^q with $\text{Validate}(EB_h^q)$ shown in Algorithm 2.2 through the following steps:

- 1) Obtain all MB_h^p whose hash values are contained in EB_h^q and execute $\text{Validate}(MB_h^p)$ to ensure all the MiniBlocks are valid.

Algorithm 2.1 MiniBlock Validation

Input: MB_h^j
Output: True or False

- 1: $\text{Hash}(\text{KB}_{h-1}), M_j, \text{ModelHash}, \text{TASK}_h \leftarrow MB_h^j$
- 2: $f, \text{Metric}(\cdot), \text{Metric}_{\min}, \text{Hash}(D_V) \leftarrow \text{TASK}_h$
- 3: $D_V \leftarrow \text{Fetch}(\text{requester}, \text{Hash}(D_V))$
- 4: $\mathbf{X}_V, \mathbf{y}_V \leftarrow D_V$
- 5: $\omega_j \leftarrow \text{Fetch}(M_j, \text{ModelHash})$
- 6: **if** $\text{Hash}(\omega_j || M_j) \neq \text{ModelHash}$ **then**
- 7: **return** False
- 8: **end if**
- 9: **if** $\text{Metric}(f(\mathbf{X}_V; \omega_j), \mathbf{y}_V) > \text{Metric}_{\min}$ **then**
- 10: **return** True
- 11: **else**
- 12: **return** False
- 13: **end if**

- 2) Check whether MB_h^p points to KB_{h-1} , the Key Block at block height $h-1$ in the local chain C_i .
- 3) Check whether the asserted metric Metric_V^q surpasses Metric_{\min} of TASK_h and equals $\text{Metric}(\text{Aggregate}(f(\mathbf{X}_V; \omega_1), \dots, f(\mathbf{X}_V; \omega_{G_{h,q}})), \mathbf{y}_V)$, where $G_{h,q}$ is the total number of MiniBlocks that EB_h^q points to.

Similar to the validation steps for MiniBlocks, the above steps are designed to ensure the performance of the ensemble models, which is a vital design goal of BagChain. However, BagChain's functionality hinges on the security and trustworthiness of the base models recorded on the blockchain. Therefore, prior to validation of the Ensemble Block EB_h^q , we safeguard the model aggregation process and combat model plagiarism and other malicious attacks by first forcing miners to download the base model parameters and verify the integrity, ownership, and performance of the base models in step 1. On the top of verified MiniBlocks, we must guarantee the ensemble models are aggregated correctly with an acceptable accuracy. We first check the miners that generate the Ensemble Block EB_h^q and all MiniBlocks MB_h^p are working on the same task by forcing all MiniBlocks MB_h^p to extend along the local chain C_i of miner M_i at block height $h-1$. To prevent the ensemble model from falling below the threshold Metric_{\min} , we require miners to verify the performance of the ensemble model on the validation dataset D_V .

C. Key Block

After miner M_i receives a new Key Block KB_h , it verifies KB_h with the operation $\text{Validate}(\text{KB}_h)$ shown in Algorithm 2.3 through the following steps:

- 1) Retrieve KB_h and its preceding Key Block KB_{h-1} from the local chain C_i . If KB_{h-1} is included in the local chain C_i , it should have been verified and the following steps can be skipped. If KB_{h-1} is not included in C_i , $\text{Validate}(\text{KB}_{h-1})$ should be executed first.
- 2) Check whether $\text{Hash}(\text{KB}_h) < \text{Target}$ holds.
- 3) Retrieve the optimal Ensemble Block EB_h^q according to the hash pointer corresponding to $\text{Metric}_{\text{best}}$ in the metric list of KB_h .

Algorithm 2.2 Ensemble Block Validation

Input: EB_h^q
Output: True or False

- 1: $MB_h^1, \dots, MB_h^{G_{h,q}}, \text{Metric}_V^q, \text{TASK}_h \leftarrow EB_h^q$
- 2: $\text{Aggregate}(\cdot) \leftarrow \text{TASK}_h$
- 3: **for** $p \leftarrow 1$ to $G_{h,q}$ **do**
- 4: **if** $\text{Validate}(MB_h^p) = \text{False}$ **or** prehash of $MB_h^p \neq \text{Hash}(\text{KB}_{h-1})$ **then**
- 5: **return** False
- 6: **end if**
- 7: **end for**
- 8: **if** $\text{Metric}_V^q = \text{Metric}(\text{Aggregate}(f(\mathbf{X}_V; \omega_1), \dots, f(\mathbf{X}_V; \omega_{G_{h,q}})), \mathbf{y}_V)$ **and** $\text{Metric}_V^q > \text{Metric}_{\min}$ **then**
- 9: **return** True
- 10: **else**
- 11: **return** False
- 12: **end if**

- 4) Execute $\text{Validate}(MB_h^p)$ to verify all the MiniBlocks in EB_h^q and whether they point to KB_{h-1} .
- 5) Aggregate the base models and evaluate the ensemble model with the test dataset D_E by calculating $\text{Metric} = \text{Metric}(\text{Aggregate}(f(\mathbf{X}_E; \omega_1), \dots, f(\mathbf{X}_E; \omega_{G_{h,q}})), \mathbf{y}_E)$.
- 6) Verify whether $\text{Metric} = \text{Metric}_E^q = \text{Metric}_{\text{best}}$, where Metric_E^q is the metric of EB_h^q in the metric list of KB_h .
- 7) Repeat step 4 and 5 for all non-optimal Ensemble Blocks $\{EB_h^r\}_{r=1}^{F_h}$ in the metric list of KB_h and verify whether $\text{Metric} = \text{Metric}_E^r \leq \text{Metric}_{\text{best}}$.
- 8) Verify whether the payload data are valid and the rewards are correctly allocated by traversing the Merkle Tree with root hash Merkle Root.

We build reliable and trustworthy data storage by designing rigorous validation steps for Key Blocks, thereby enabling miners to upload training outcomes and requesters to receive desired ML models even in an untrustworthy environment. Basically, we ensure BagChain's consistency and immutability with the PoW validation steps and the hash chain structure of Key Blocks. Then, we distinguish BagChain from classic PoW systems with the recursive validation of the Ensemble Blocks and MiniBlocks. The recursive validation procedures ensure the correctness and accuracy of all the ensemble models and their base models by traversing BagChain's three-layer chain structure and verifying all the models involved.

Moreover, we include the incentive mechanism in the validation procedures of Key Blocks. Recall that the training rewards are evenly distributed to the miners that generate the base models of the winning ensemble model, we add steps that check training reward allocation and invalidate Key Blocks that pick an incorrect winning ensemble block by verifying the metric of the winning ensemble model against the claimed metric $\text{Metric}_{\text{best}}$.

All above, the validation procedures of Key Blocks, along with the fork resolution rule that retains the Key Block with the optimal $\text{Metric}_{\text{best}}$ in the local chain C_i , enable requesters to download the best possible ensemble model with the information recorded on the main chain.

Algorithm 2.3 Key Block Validation

Input: KB_h **Output:** True or False

```

1:  $EB_h^1, \dots, EB_h^{F_h}, \text{Metric}_{best}, \text{TASK}_h \leftarrow KB_h$ 
2:  $\text{Aggregate}(\cdot), \text{Hash}(D_E) \leftarrow \text{TASK}_h$ 
3:  $D_E \leftarrow \text{Fetch}(\text{requester}, \text{Hash}(D_E))$ 
4:  $X_E, y_E \leftarrow D_E$ 
5: if  $\text{Hash}(KB_h) \geq \text{Target}$  then
6:   return False
7: end if
8: for  $r \leftarrow 1$  to  $F_h$  do
9:    $MB_h^1, \dots, MB_h^{G_{h,r}} \leftarrow EB_h^r$ 
10:  for  $p \leftarrow 1$  to  $G_{h,r}$  do
11:    if  $\text{Validate}(MB_h^p) = \text{False}$  or prehash of  $MB_h^p \neq$ 
       $\text{Hash}(KB_{h-1})$  then
12:      return False
13:    end if
14:  end for
15:  if  $\text{Metric}_E^r \neq \text{Metric}(\text{Aggregate}(f(X_E; \omega_1), \dots,$ 
     $f(X_E; \omega_{G_{h,r}}), y_E)$  or  $\text{Metric}_E^r > \text{Metric}_{best}$  then
16:    return False
17:  end if
18: end for
19: if  $\text{Metric}_{best}$  in  $\{\text{Metric}_E^r\}_{r=1}^{F_h}$  and payload data in the
    Merkle Tree are valid then
20:   return True
21: else
22:   return False
23: end if

```

V. CROSS FORK SHARING

In practical networks, miners may have different blockchain visions due to the propagation delay or malicious attacks, and they may generate different Key Blocks and cause blockchain forking. Multiple Key Blocks may lead miners to work on different forks and split the blockchain network into disjoint partitions mining on separate Key Blocks. Since miners strictly stick to the validation procedures in Section IV, the base models are only available for model aggregation on the top of the same Key Block and are discarded by the miners working on another. Consequently, the miners in each partition can only aggregate a limited portion of MiniBlocks, wasting base models and computing power. It also degrades the performance of the final ensemble model, as further shown in Fig. 11 in the simulation. The above phenomenon is referred to as "computing power splitting" in our paper.

We visualize the above phenomenon in Fig. 3. At block height h , there are two different Key Blocks, denoted as \widetilde{KB}_h and KB_h , and their child Key Blocks, denoted as \widetilde{KB}_{h+1} and KB_{h+1} . The Key Blocks KB_h and KB_{h+1} are on the main chain while \widetilde{KB}_h and \widetilde{KB}_{h+1} are forks. Note that the Ensemble Block \widetilde{EB}_{h+1}^1 on the fork points to two MiniBlocks and the Ensemble Block EB_{h+1}^1 on the main chain points to three MiniBlocks. Hence, the ensemble model corresponding to EB_{h+1}^1 does not fully utilize all the base models and thus the computing power splits at height h . Obviously, the

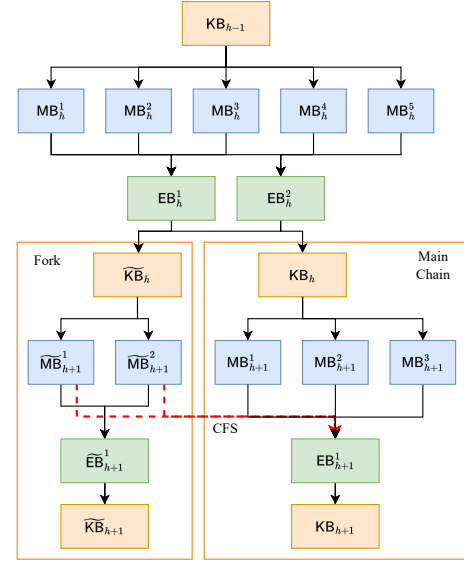


Fig. 3. Blockchain fork and the proposed cross fork sharing mechanism.

performance of the ensemble models is positively related to the number of aggregated base models. As "computing power splitting" occurs, some available computing power is wasted in generating the base models on the fork and thus the performance of the final ensemble model degrades. This is why in Section VII-D the network delay affects the model accuracy on the test dataset. Though the requester could download the base models from the miners producing the two MiniBlocks \widetilde{MB}_{h+1}^1 and \widetilde{MB}_{h+1}^2 on the fork \widetilde{KB}_{h+1} to improve ensemble model quality, these two MiniBlocks \widetilde{MB}_{h+1}^1 and \widetilde{MB}_{h+1}^2 are invalid on the main chain KB_{h+1} according to Algorithm 2.3. Also, the miners who generate \widetilde{MB}_{h+1}^1 and \widetilde{MB}_{h+1}^2 are unlikely to share their base models with the requester if they are not rewarded on the main chain.

To make BagChain more robust to "computing power splitting", we propose a cross fork sharing (CFS) mechanism to enable model sharing among the main chain and different forks. In the CFS mechanism, we remove the restrictions on the prehash of MB_h^p in line 4 of Algorithm 1.2 and line 4 of Algorithm 2.2 and allow miners to leverage more base models they have received. As depicted in Fig. 3, with the CFS mechanism, the miner generating \widetilde{EB}_{h+1}^1 can aggregate the base models on different forks such as \widetilde{MB}_{h+1}^1 and \widetilde{MB}_{h+1}^2 if the following conditions are fulfilled:

- 1) All MiniBlocks to be included in \widetilde{EB}_{h+1}^1 should be at the same block height and have the same task ID $\text{Hash}(\text{TASK}_{h+1})$. Otherwise, the metrics of their base models can not be compared since the test datasets of different tasks differ.
- 2) The aggregated base models should be unique in case any miner submits duplicate base models on different forks.
- 3) The performance metrics of all aggregated base models must satisfy the minimum requirement Metric_{min} .

Since different MiniBlocks might point to different Key Blocks at the same block height, we employ a majority voting rule

to determine which Key block is on the main chain. Every valid MiniBlock is viewed as a “vote” for the Key Block that the MiniBlock points to because the MiniBlock represents a certain amount of time-consuming base model training and Key Block validation work. Therefore, the hash value of the parent Key Block should be derived from the majority voting of the MiniBlocks that the winning Ensemble Block points to. For instance, in Fig. 3, the prehash of KB_{h+1} should be $\text{Hash}(KB_h)$ since among the MiniBlocks that the winning Ensemble Block EB_{h+1}^1 points to, three MiniBlocks “vote” for KB_h while only two MiniBlocks “vote” for \widetilde{KB}_h . The performance of the CFS mechanism in high-latency networks is further shown in Section VII-D.

VI. PERFORMANCE AND SECURITY

A. Underfitting and Overfitting

In this section, we will dive deep into several performance and security issues of BagChain. To prevent base models from underfitting, we introduce the validation dataset and a threshold Metric_{\min} in BagChain. MiniBlocks will not be included in any valid Ensemble Block unless the base models corresponding to the MiniBlocks satisfy the metric threshold Metric_{\min} of the ML task on the validation dataset. In this way, unqualified base models are filtered out.

Overfitting is a more important issue that needs to be particularly considered for learning-based useful work proof. Lazy nodes may simply train models by overfitting the samples in the test dataset, which significantly compromises the learning performance. Therefore, in BagChain, miners evaluate ensemble models on test datasets to minimize the generalization error of the ensemble models of BagChain. In Phase III (Key Block Generation), the requester discloses a test dataset different from the validation dataset, and the miners evaluate all the ensemble models collected in Phase II (Ensemble Block Generation) on the test dataset. The miners overfitting the ensemble models on the validation dataset reap no benefits since the ensemble models overfitting on the validation dataset have no advantage over the other ensemble models on the test dataset.

B. Model Plagiarism

Model plagiarism is another important issue of PoUW protocols like BagChain where lazy nodes may steal base models from other miners. It discourages honest miners from contributing base models in BagChain. We address this issue via the model submitting scheme illustrated in Fig. 4. The hash values of the base models, i.e., ModelHash, are submitted in MiniBlocks first, and miners stop accepting MiniBlocks after the validation dataset is published. The miners training the base models and generating MiniBlocks do not accept incoming model download requests until the validation dataset is published. Hence, the lazy miners who attempt to steal base models cannot download them from other miners before validation dataset disclosure, and any base model submitted with a MiniBlock will be rejected by honest miners after the validation dataset is published.

However, even with the model submitting scheme, lazy miners can copy the hash value of ω_j from miner M_j 's

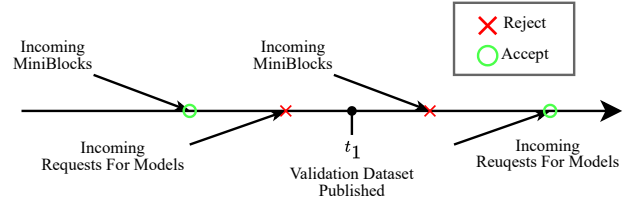


Fig. 4. Model submitting scheme designed in BagChain workflow to combat ML model plagiarism.

MiniBlock as the ModelHash of their own MiniBlocks and upload ω_j as if ω_i is their own base model after the validation dataset is published. To close the loophole, we define ModelHash as $\text{Hash}(\omega_i || M_i)$ to conceal the actual hash value of ω_i and bind the identity of miner M_i to ω_i . In this way, lazy miners' MiniBlocks containing a copied ModelHash and a mismatching miner ID will fail to pass the MiniBlock validation step in line 6 of Algorithm 2.1.

C. Dataset Leakage Caused by Forking

As a distributed system, blockchain forking caused by network delays or attackers may pose potential risks of leaking validation and test datasets since two different subsets of miners might execute different tasks at the same block height. Fig. 5 depicts the possible blockchain structures when blockchain forking occurs. As shown in Fig. 5(a) and 5(b), The two types of blockchain forks might lead to dataset leaks.

In Fig. 5(a), after TASK_h is completed at block height h , a fork \widetilde{KB}_h is created. For the miners accepting \widetilde{KB}_h as the main chain, TASK_{h+2} is executed in advance, resulting in early publication of the validation and test datasets at block height $h + 1$. Moreover, the miners accepting \widetilde{KB}_h as the main chain may train base models for TASK_{h+2} . In this case, these miners may train the base models on the test dataset published at block height $h + 1$ for better scores on the test dataset. However, they actually overfit the test dataset and are against the intention of introducing validation and test datasets into BagChain. If only a minority of miners train and aggregate models on the fork, the produced ensemble model may underperform the ensemble model on the main chain. Such deterioration in ensemble model performance on the test dataset is undesired for requesters.

In Fig. 5(b), after TASK_h is completed at block height h , TASK_{h+1} is generated by the requester, included in the fork \widetilde{KB}_h , and executed at block height $h+1$. This means TASK_{h+1} is executed before being confirmed in any Key Block on the main chain, and thus its execution is not recorded on the main chain. As a result, the training fees of TASK_{h+1} are not deducted from the requester's account on the main chain, and the miners working on the fork \widetilde{KB}_h get nothing in return.

Consequently, concerned with the above situations, requesters will hesitate to publish their datasets until they confirm that no fork is created in the blockchain system, which delays dataset publication and impairs BagChain's performance, especially in harsh network environments.

To tackle the issue, we set up a first-in-first-out queue in Key Blocks to record upcoming tasks by storing their IDs. Whenever miners start training base models, they pick up

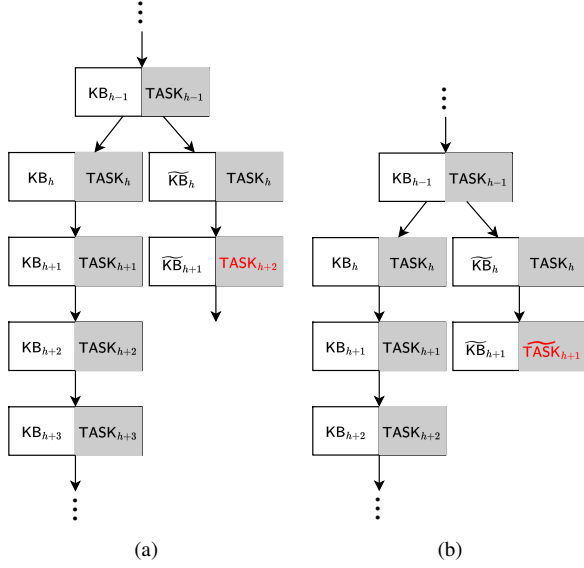


Fig. 5. Two possible situations when dataset leakage occurs in BagChain. (a) Early execution of a task on the main chain. (b) Execution of a task not recorded on the main chain.

the first item in the task queue as the current task. When generating Key Blocks, they remove the first item from the original task queue and append a new ML task to the tail of the new task queue. The new ML task can be either randomly drawn from miners’ task transaction pool or prioritized based on the training fees offered by requesters. If a task enters a task queue of length Q , the execution of the task will be scheduled Q block heights later, even if multiple forks are created. In this way, the tasks executed on different forks at the same block height remain unified. The choice of task queue length Q is a trade-off since Q should be upper bounded to limit the size of Key Blocks and be lower bounded to guarantee sufficient robustness to blockchain forking.

Last but not least, the task queue also benefits requesters in the following aspects. First, with the task queue, they can predict the tasks to be executed at the following block heights and prepare to distribute the public training dataset in advance. Second, the task queue can improve the effectiveness of the proposed CFS mechanism and thus boost the performance of the ensemble models. Actually, as long as the task queue is long enough, the task queue guarantees task consistency across different blockchain forks and ensures the same task is executed at the same block height, enabling cross-fork base model sharing (see condition 1 in Section V). In this case, most base models generated at the same block height can be aggregated into the Ensemble Block in Phase II, which reduces computing power waste in BagChain.

VII. CHAINXIM-BASED EXPERIMENTS

A. Simulation Setup

We realize and evaluate the framework of BagChain based on ChainXim,¹ a blockchain simulator based on a discrete-time Byzantine setting [33]. In ChainXim, time is segmented into many intervals as “rounds”. As Fig. 6(a) illustrates, every miner validates the received blocks and merges valid ones into

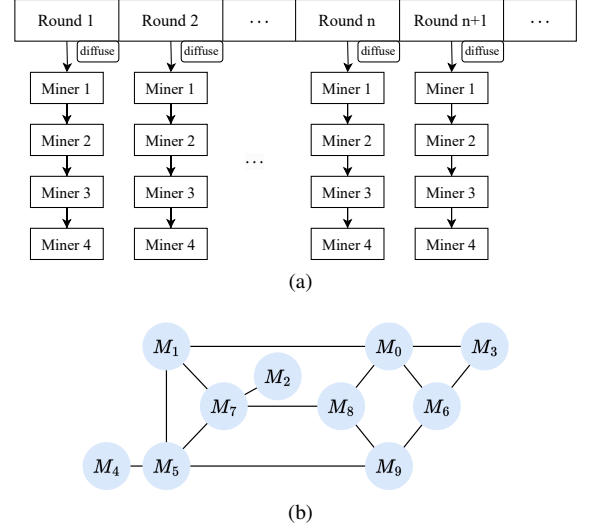


Fig. 6. Overview of ChainXim’s internal mechanisms. (a) Discrete-time simulation workflow utilizing “round” as the minimum time unit for simulating miners’ actions and block dissemination. (b) Topology of the mesh network used in Fig. 11 and Fig. 12.

the local chain. It attempts to generate new blocks to the main chain in its own view and diffuses the newly generated blocks (if any) via the network layer. ChainXim supports various user-configured network models to simulate different scenarios. Specifically, the simulations in Section VII-D use the topology depicted in Fig. 6(b).

Our simulations are based on several widely used image classification tasks including MNIST [34], CIFAR-10 [35], SVHN [36], and FEMNIST [37]. Our simulation experiments not only consider various ML tasks but also different types of base models including decision trees and a series of convolutional neural networks (CNNs). Decision trees are classic ML classifiers frequently used in conjunction with ensemble learning techniques like bagging [31] and random forest, and we use the implementation in scikit-learn. The CNNs include LeNet [38], ResNet18 [39], DenseNet [40], and MobileNetV2 [41]. All neural networks are implemented with Pytorch and trained with a learning rate of 0.001.

For a given ML task, we construct the public training dataset D_T , the validation dataset D_V , and the test dataset D_E from its original datasets. We randomly select $|\hat{D}_E|/2$ samples in the original test dataset as the new validation dataset D_V in Phase II and set the rest as the new test dataset D_E in Phase III. Furthermore, we split the original training dataset \hat{D}_T into a public training dataset D_T and several private datasets D_{M_i} assigned to miners. In the IID setting, we split the datasets evenly into homogeneous subsets, whereas in the non-IID setting, we adopt the experimental setup in [42] to introduce distribution-based label heterogeneity and real-world feature heterogeneity into the private datasets. More details about dataset setups are presented in the Appendix.

The model accuracy, defined as the ratio of the correctly classified samples to the total number of samples in a dataset, is used as the performance metric to assess BagChain. During the simulations, ChainXim records the accuracy of the ensemble models and the corresponding base models on the test dataset D_E at each block height.

¹ChainXim is available at <https://github.com/ChainXim-Team/ChainXim>.

TABLE I
TEST DATASET ACCURACY OF THE BASE AND ENSEMBLE MODELS
GENERATED IN BAGCHAIN

Dataset	Model	Public (%)	Base Min~Max (%)	BagChain (%)
MNIST	Decision Tree	81.50	80.58~81.92	91.66
CIFAR-10	LeNet	50.48	44.48~49.72	60.04
	ResNet18	68.24	65.10~70.22	76.70
	DenseNet	71.88	70.02~73.76	81.58
	MobileNetV2	60.70	58.46~61.70	72.58
SVHN	LeNet	80.65	81.75~83.78	89.02
	ResNet18	88.62	86.95~92.03	96.00
	DenseNet	91.20	90.26~92.11	95.29
	MobileNetV2	89.38	86.21~90.28	94.08
FEMNIST	LeNet	77.02	74.70~77.51	83.39
	ResNet18	75.82	76.79~80.31	85.07
	DenseNet	74.22	74.10~81.10	85.82
	MobileNetV2	76.13	75.63~78.45	85.09

The size of MiniBlocks and Ensemble Blocks is set to 2 MB and the size of Key Blocks is 6 MB by default. The corresponding propagation delay can be calculated according to the bandwidth of the link. For example, in the fully-connected network, it takes 12 rounds for a block to reach all miners. In our simulation, Phase I and Phase II are set to the fixed 100 rounds and 10 rounds, respectively. In other words, the requester publishes the validation dataset 100 rounds after Phase I starts and publishes the test dataset 10 rounds after Phase II starts.

We set $\text{Target} = 2^{244} - 1$ to safeguard the Key Block and reduce the probability of forking. We implement $\text{Hash}(\cdot)$ with the SHA256 hash function in ChainXim, so the probability that a miner finds a valid nonce satisfying $\text{Hash}(\text{KB}_h) < \text{Target}$ after q mining attempts in each round is $1 - (1 - \text{Target}/2^{256})^q$ ($q = 1$ in our simulation). Obviously, a smaller Target, i.e., a larger difficulty, reduces the forking probability but also results in a higher Key Block mining delay.

B. BagChain Performance for Different ML Tasks

In this section, we compare the performance of the ensemble models generated by BagChain with that of the base models from the ChainXim-based simulations in a fully connected network with 10 miners in an IID setting. As shown in Fig. 7, “BagChain”, “Base Model”, and “Public” represent the ensemble models based on the proposed BagChain, the base models trained on every miner’s local datasets D_{T_i} , and a dummy model directly trained on the public training dataset D_T , respectively. The scattered points correspond to the accuracies of every miner’s local base models in the network, which is illustrated as the transparent area to show the upper and lower bounds of local base models. The different colors correspond to the cases where the base models are trained for 10, 20, and 30 epochs, respectively.

From Fig. 7, we observe that the ensemble models outperform the base models trained on every miner’s local dataset and also the dummy model trained on the public dataset. This phenomenon highlights BagChain’s capability to improve prediction accuracy through the collective wisdom of multiple expert systems trained on disjoint private and valuable datasets, thereby achieving better performance than any single model trained on every miner’s private datasets

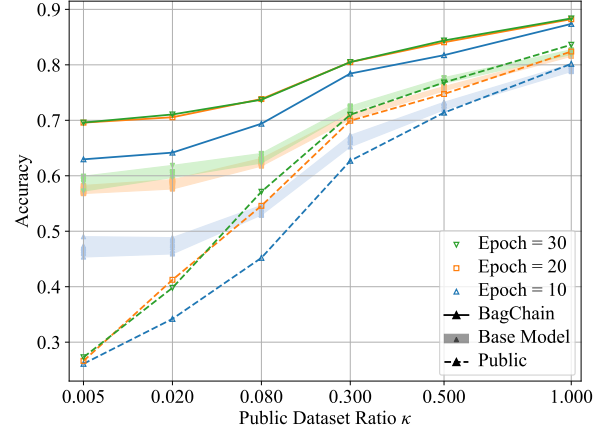


Fig. 7. Performance boost of BagChain compared with base models in a fully-connected network with $N = \varphi = 10$. (The dataset is CIFAR-10 and the base model is ResNet18.)

or the requester’s limited data samples. Note that BagChain does not require miners to reveal or exchange the raw dataset for privacy protection. Not surprisingly, the accuracy of base and ensemble models in BagChain increases as the public dataset ratio κ rises, i.e., more samples in the public training dataset D_T . However, even when $\kappa = 1$, i.e., all the models are based on the same dataset, the ensemble model of BagChain still outperforms other approaches. Therefore, apart from the knowledge from private datasets, BagChain’s accuracy-augmenting capability also benefits from multiple miners’ computing power and the performance gain of the Bagging algorithm, i.e., aggregation of multiple expert models. Furthermore, we would like to highlight that BagChain does not rely on well-trained base models. As shown in Fig. 7, around 20 epochs are sufficient to train base models since the ensemble models corresponding to the base models trained by 20 and 30 epochs exhibit a negligible performance gap. Hence, BagChain allows mobile devices, which have local data samples but are resource-constrained, to participate in model training without competing to fine-tune ML models. Therefore, as shown in Fig. 7, BagChain can turn possibly weak base models into strong ensemble models by utilizing distributed computing power and every node’s local data without affecting individual privacy.

Furthermore, in Table I, we illustrate BagChain’s capability and adaptability for various ML tasks using different base models. In this experiment, BagChain is simulated in a fully-connected network with the public dataset ratio $\kappa = 0.1$. The column labeled “Base Min~Max (%)” provides the range of the accuracy of the miner’s base models. From Table I, BagChain has about 3%~20% accuracy improvement compared with all the base models and the models training solely with the public dataset for all tested models and datasets. This demonstrates BagChain’s generalization performance in various ML tasks.

C. BagChain Performance In the Non-IID Setting

In this section, we assess the performance of BagChain by taking into account two different types of non-IIDness. In Fig. 8(a)-8(c), we construct label distribution heterogeneity in the datasets of MNIST, CIFAR-10, and SVHN, respectively. In Fig. 8(d), we leverage the inherent feature heterogeneity

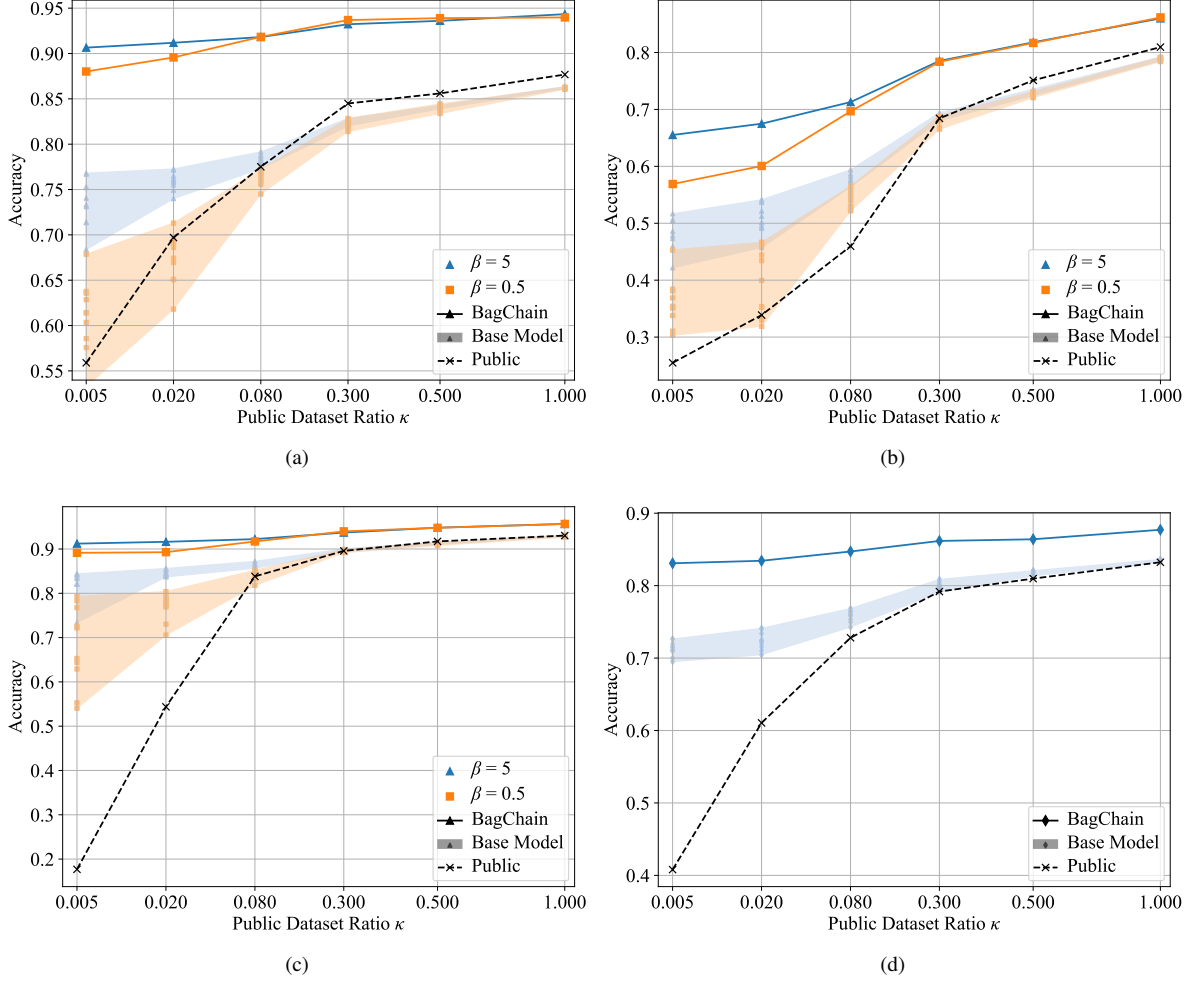


Fig. 8. Performance boost of BagChain compared with base models under different types and degrees of data heterogeneity in a fully-connected network with $N = \varphi = 10$. Every CNN is trained for 10 epochs. (a) MNIST + Decision Tree. (b) CIFAR-10 + ResNet18. (c) SVHN + ResNet18. (d) FEMNIST + ResNet18.

in FEMNIST. The simulation results consistently show the accuracy advantages of BagChain over the base models and also the dummy "public" model. Therefore, BagChain is effective and adaptable to different non-IID ML tasks. Notably, Fig. 8(d) shows that BagChain performs effectively even when the base models are trained on partitioned FEMNIST, where the features in each miner's dataset are handwritten digits from distinct groups of writers, underscoring BagChain's robustness to feature distribution heterogeneity.

Specifically, in Fig. 8(a)-8(c), we show the intensity of non-IIDness in private datasets across different miners via the concentration parameter β . The concentration parameter β of the Dirichlet distribution $Dir(\beta)$ controls the intensity of label distribution heterogeneity, and a smaller β represents a higher degree of non-IIDness. The performance of base models is significantly affected by the smaller concentration parameter β , and meanwhile, the ensemble models generated by BagChain remain robust against heterogeneity, highlighting BagChain's effectiveness in the non-IID setting. Furthermore, from Fig. 8(a)-8(c), we observe that the gap between the two curves corresponding to $\beta = 5$ and $\beta = 0.5$ narrows as the public dataset ratio κ increases. This is because the public data samples help balance the label distribution in miners'

local datasets and reduce the error of each base model.

We further illustrate BagChain's effectiveness under different degrees of label distribution heterogeneity in Fig. 9. In this figure, the different colors correspond to different public dataset ratios $\kappa = 0.02, 0.1$, and 0.2 , respectively. Similarly, all the ensemble models in BagChain achieve performance advantage over the base models, even with severe label distribution heterogeneity, indicating BagChain's effectiveness in the non-IID setting. Also, as the public dataset ratio κ increases from 0.02 to 0.2 , the model accuracy curve flattens. When the public dataset ratio κ equals 0.2 , we observe no significant accuracy drop as the concentration parameter β varies within the range $[0.1, 15]$. As explained above, this is because more public data helps reduce the impact of label distribution heterogeneity and improve the performance of both base models and ensemble models. Given the pervasive data heterogeneity in real-world distributed learning scenarios with multiple data sources, the above results demonstrate that BagChain is both practical and effective for such applications.

D. BagChain Robustness against Different Network Conditions

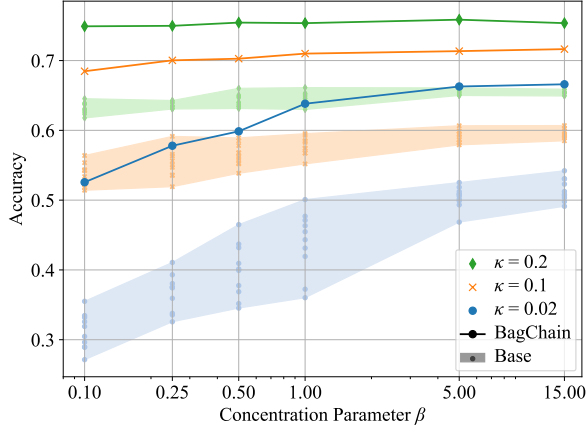


Fig. 9. Model performance under different public dataset ratios κ and concentration parameters β . (The dataset is CIFAR-10 and the base model is ResNet18. Every base model is trained for 10 epochs.)

In this section, we explore how network scale, network connectivity, and the amount of private data impact the performance of BagChain. In Fig. 10, the x-axis “Miner Number” measures the scale of the blockchain network. The “Fully-connected Network” and “Mesh Network” in the legend are the fully-connected network and mesh networks. In the fully-connected network, each miner can communicate with all other miners. On the contrary, in the mesh networks, each miner connects with only a subset of the miners, and the topologies of the mesh networks are Erdős-Rényi graphs randomly generated with networkx. In both network models, the bandwidth between connected miners is 0.5 MB per round. The different colors in Fig. 10 correspond to different private dataset ratios $\zeta = 0.04$ and 0.06 , which controls the number of samples in miners’ private datasets.

Fig. 10 shows that BagChain is scalable since its accuracy increases with more miners. This is because, as the network scales, more private data and computing power are invested in training base models, and more base models are aggregated. Also, a higher private dataset ratio ζ significantly boosts the accuracy of the ensemble models generated in BagChain. Hence, BagChain is more accurate if miners contribute more private data to collaborative ML task training. Moreover, the negligible gap between the accuracy in a fully connected network (solid lines) and the one in a mesh network (dashed lines) in Fig. 10 indicates that BagChain experiences minor performance degradation in a loosely connected blockchain network. Notably, even in a 25-node mesh network with long-tailed propagation latency, the ensemble models in BagChain remain accurate, highlighting its robustness against weak connectivity and harsh network conditions.

Furthermore, we investigate the performance of CFS by considering blockchain forking to show the efficacy of the CFS mechanism. This experiment uses a mesh network model with the topology depicted in Fig. 6(b). As shown in Fig. 11, “w/o CFS” represents the original BagChain scheme without CFS while “w/ CFS” represents the improved BagChain scheme with CFS. The x-axis “Network Delay” means the transmission delay for each Key Block on each network connection. The y-axis “MiniBlock Wastage” is the average

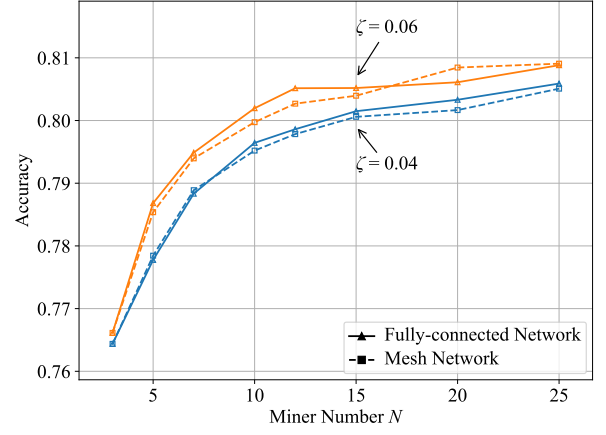


Fig. 10. Model performance in different network scale. (The dataset is CIFAR-10 and the base model is ResNet18. Every base model is trained for 10 epochs and the public dataset ratio κ equals 0.4.)

difference between the total number of MiniBlocks and the number of MiniBlocks used by the winning Ensemble Block.

Fig. 11 illustrates the impact of network delay on MiniBlock wastage and the accuracy of the ensemble models. From the curve marked “w/o CFS”, we observe a decrease in the accuracy of the ensemble models generated in ChainXim as the network delay increases. Also, MiniBlock wastage rises and ensemble model accuracy drops as the network latency increases. This is because fewer base models can be utilized in model aggregation in Phase II since frequent blockchain forking causes the “computing power splitting” phenomenon described in Section V. In a blockchain network with high network delay, frequent blockchain forking leads miners to generate MiniBlocks on different blockchain forks, which cannot be shared among different forks. The crux of the problem here is that the MiniBlocks a miner can utilize are limited to those pointing to the same Key Block when generating an Ensemble Block without using the CFS mechanism. It reduces the base models available for model aggregation and causes computing power waste in Phase II. In the curve marked “w/ CFS”, the accuracy of the ensemble models drops slightly below 0.94 as the network delay increases from 2 rounds to 32 rounds, and MiniBlock wastage is almost negligible when the network delay is fewer than 32 rounds. This is because the CFS mechanism improves BagChain by making all the MiniBlocks on different forks available for model aggregation in Phase II. The more base models are aggregated in ensemble models, the better performance the ensemble models can achieve. Thereby, the proposed CFS mechanism can improve ensemble model performance by avoiding computing power wastage and maximizing the number of aggregated base models in ensemble models.

Fig. 12 further compares the actual accuracy of the ensemble models with their best possible accuracy. The actual accuracy is the accuracy of the winning ensemble models in Key Blocks, while the best possible accuracy is the performance metric of an ideal ensemble model aggregating all the base models available for each task. The best possible accuracy is usually unattainable in BagChain because the network delay may waste computing power (see Section V) or untimely exchange

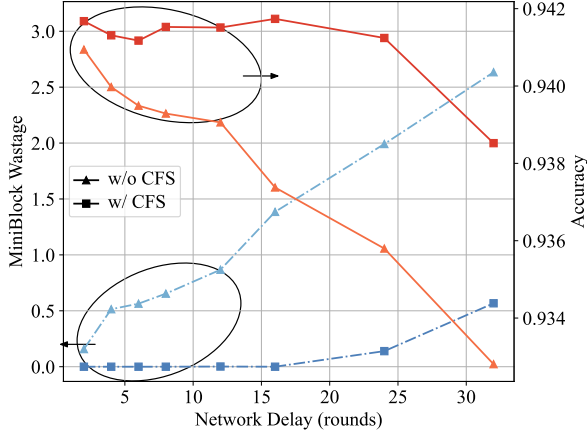


Fig. 11. Average number of wasted MiniBlocks and accuracy of the ensemble models generated in BagChain under different network delays. (The dataset is MNIST and the base model is a decision tree.)

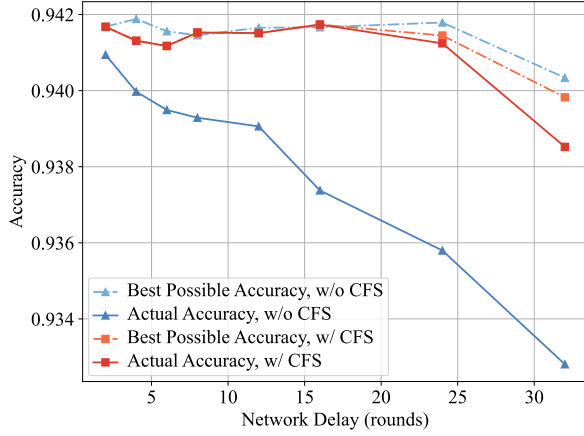


Fig. 12. Actual accuracy and best possible accuracy of the ensemble models generated in BagChain under different network delays. (The dataset is MNIST and the base model is a decision tree.)

of MiniBlocks and base models among miners. From Fig. 12, compared with BagChain without CFS, the actual accuracy of BagChain with CFS is closer to the best possible accuracy. The benefit of CFS becomes more significant as the network delay increases. Both Fig. 11 and Fig. 12 illustrate that the proposed CFS mechanism can utilize computing power more efficiently and enhance BagChain’s robustness to blockchain forking and computing power splitting.

VIII. CONCLUSION

In this paper, we propose and design BagChain, a bagging-based dual-functional blockchain framework, to leverage both the computing power and private data in a permissionless blockchain network. We record the results of base model training, base model aggregation, and ensemble model ranking in MiniBlocks, Ensemble Blocks, and Key Blocks, respectively, and embed the bagging algorithm into the generation and verification procedures of the corresponding three types of blocks. We further propose the CFS mechanism to maximize base model utilization, reduce computing power waste, and improve BagChain’s performance. We conduct comprehensive experiments with ChainXim to demonstrate the efficacy of BagChain for various ML tasks under different data

TABLE II
NUMBER OF SAMPLES IN EACH DATASET SPLIT FROM THE ORIGINAL TRAINING DATASET IN THE IID SETTING. (MINER NUMBER $N = \varphi = 10$.)

Task	MNIST	CIFAR-10	SVHN
Total Training Samples $ \hat{D}_T $	60000	50000	73257
Public Dataset Ratio κ	0.4		
Public Dataset $ D_T = \kappa \hat{D}_T $	24000	20000	29302
Private Dataset Ratio $\zeta = D_{M_i} / \hat{D}_T $	0.06		
Private Dataset $ D_P = \hat{D}_T - D_T $	36000	30000	43955
Private Dataset Per Miner $ D_{M_i} = D_P /N$	3600	3000	4395

heterogeneity settings and network conditions. The simulation results in the IID setting highlight the performance superiority of the ensemble models in BagChain compared with the models trained solely with miners’ restricted datasets or requesters’ public datasets. The experiments in the non-IID setting demonstrate that the ensemble models generated in BagChain can achieve desirable performance even if the label and feature distributions in miners’ private datasets are heterogeneous. By testing BagChain under different network conditions, we find that BagChain is scalable and generates better ensemble models if larger computing power and more private data samples are involved in base model training. Thanks to the proposed CFS mechanism, BagChain exhibits strong robustness against harsh network environments with poor connectivity and high latency.

APPENDIX

In the appendix, we would like to explain how we set up the datasets in the simulations. The local dataset D_{T_i} of miner M_i is the union of the public training dataset D_T and the private dataset D_{M_i} . All miners share the same public training dataset D_T in each ML task, and the size of the public training dataset $|D_T|$ is controlled by public dataset ratio κ , defined as $\kappa = |D_T|/|\hat{D}_T|$. The way to create the private dataset D_{M_i} differs in IID and non-IID settings.

In the IID setting, we split the original training dataset \hat{D}_T into a public part D_T and a private part, which is then evenly partitioned into φ subsets, denoted as D_{S_i} for $i = 1, \dots, \varphi$. (If $\varphi \geq N$, D_{S_i} is assigned to miner M_i ($D_{M_i} = D_{S_i}$) for $i = 1, \dots, N$. Otherwise, D_{S_j} is assigned to miner M_i ($D_{M_i} = D_{S_j}$), in which j equals i for $i \leq \varphi$ and is randomly selected from $\{1, 2, \dots, \varphi\}$ for $i > \varphi$.) Private dataset ratio ζ is defined as $\zeta = |D_{S_i}|/|\hat{D}_T|$, controlling the size of miners’ private datasets $|D_{M_i}|$. When the public dataset ratio κ is 0.4 and private dataset ratio ζ is 0.06, the number of samples in the datasets mentioned above are shown in Table II.

In the non-IID setting, we experiment with two distinct types of non-IIDness: label distribution heterogeneity and feature distribution heterogeneity [42]. We curate datasets with heterogeneous label distributions from balanced datasets including MNIST, CIFAR-10, and SVHN to simulate label distribution heterogeneity, and we utilize the inherent heterogeneity in the feature distribution of the data samples in FEMNIST to simulate feature distribution heterogeneity.

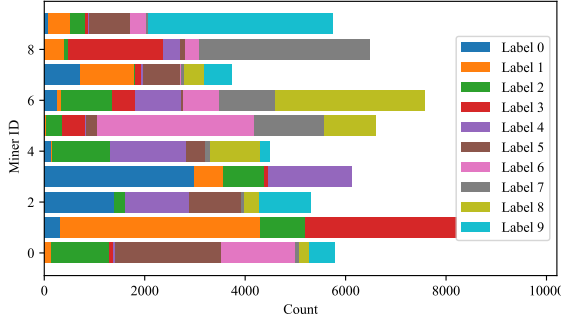


Fig. 13. Label distribution of each miner's private datasets when splitting non-IID subsets from CIFAR-10 with $\beta = 0.5$ and $N = 10$.

MNIST, CIFAR-10, and SVHN are split into a public part D_T and a private part D_P . Suppose there are L classes in the original training dataset \hat{D}_T , and let the subset D_{P_k} contain all samples of class k in the private dataset D_P . We draw a probability mass function $p_k : \{1, \dots, N\} \rightarrow [0, 1]$ from the Dirichlet distribution $\text{Dir}_N(\beta)$ and then randomly partition the subset D_{P_k} into N subsets $\{D_{P_{k,j}}\}_{j=1}^N$, where each $D_{P_{k,j}}$ accounts for $p_k(j)$ of D_{P_k} [43]. The private datasets D_{M_j} assigned to miner M_j is the union of $\{D_{k,j}\}_{k=1}^L$. The concentration parameter β of the Dirichlet distribution $\text{Dir}_N(\beta)$ controls the degree of label distribution heterogeneity, where a lower β results in a higher degree of label imbalance. As an example, in Fig. 13, we depict the label distribution of each miner's private dataset when splitting CIFAR-10 into non-IID subsets with concentration parameter $\beta = 0.5$. For FEMNIST, the training samples are the handwritten digits grouped into non-overlapping subsets D_{S_i} based on their writers. The public dataset D_T is constructed by randomly extracting $|D_T|/N$ samples from each D_{S_i} , and the private datasets D_{M_i} contain the remaining samples in each subset D_{S_i} .

REFERENCES

- [1] H. He and E. A. Garcia, "Learning from imbalanced data," *IEEE Trans. Knowl. Data Eng.*, vol. 21, no. 9, pp. 1263–1284, Sep. 2009.
- [2] B. McMahan, E. Moore, D. Ramage, S. Hampson, and B. A. y. Arcas, "Communication-efficient learning of deep networks from decentralized data," in *Proc. 20th Int. Conf. Artif. Intell. Statist.*, Fort Lauderdale, FL, USA, Apr. 2017, pp. 1273–1282.
- [3] L. Georgopoulos and M. Hasler, "Distributed machine learning in networks by consensus," *Neurocomputing*, vol. 124, pp. 2–12, Jan. 2014.
- [4] P. Kairouz *et al.*, "Advances and open problems in federated learning," *Found. Trends Mach. Learn.*, vol. 14, no. 1–2, pp. 1–210, Jun. 2021.
- [5] X. Ling, J. Wang, Y. Le, Z. Ding, and X. Gao, "Blockchain radio access network beyond 5G," *IEEE Wireless Commun.*, vol. 27, no. 6, pp. 160–168, Dec. 2020.
- [6] W. Cao, X. Ling, J. Wang, X. Gao, and Z. Ding, "Optimization-based proof of useful work: Framework, modeling, and security analysis," May 2024.
- [7] X. Ling, Y. Le, J. Wang, Y. Huang, and X. You, "Trust and trustworthiness in information and communications technologies," *IEEE Wireless Commun.*, vol. 32, no. 2, pp. 84–92, Apr. 2025.
- [8] B. Li, C. Chenli, X. Xu, Y. Shi, and T. Jung, "DLBC: A deep learning-based consensus in blockchains for deep learning services," *arXiv preprint arXiv:1904.07349*, Jan. 2020.
- [9] C. Qiu, X. Wang, H. Yao, J. Du, F. R. Yu, and S. Guo, "Networking integrated cloud-edge-end in IoT: A blockchain-assisted collective Q-learning approach," *IEEE Internet Things J.*, vol. 8, no. 16, pp. 12 694–12 704, Aug. 2021.
- [10] B. Li, Q. Lu, W. Jiang, T. Jung, and Y. Shi, "A collaboration strategy in the mining pool for proof-of-neural-architecture consensus," *Blockchain: Res. Appl.*, vol. 3, no. 4, p. 100089, Dec. 2022.
- [11] T. Xiang, H. Zeng, B. Chen, and S. Guo, "BMIF: Privacy-preserving blockchain-based medical image fusion," *ACM Trans. Multimedia Comput. Commun. Appl.*, vol. 19, no. 1s, pp. 1–23, Jan. 2023.
- [12] F. Bravo-Marquez, S. Reeves, and M. Ugarte, "Proof-of-learning: A blockchain consensus mechanism based on machine learning competitions," in *Proc. 2019 IEEE Int. Conf. Decentralized Appl. Infrastruct. (DAPPCON)*, Newark, CA, USA, Apr. 2019, pp. 119–124.
- [13] C. Chenli, B. Li, Y. Shi, and T. Jung, "Energy-recycling blockchain with proof-of-deep-learning," in *Proc. 2019 IEEE Int. Conf. Blockchain Cryptocurrency (ICBC)*, Seoul, KR, May 2019, pp. 19–23.
- [14] J. Kang, Z. Xiong, D. Niyato, Y. Zou, Y. Zhang, and M. Guizani, "Reliable federated learning for mobile networks," *IEEE Wirel. Commun.*, vol. 27, no. 2, pp. 72–80, Apr. 2020.
- [15] Z. Li, H. Yu, T. Zhou, L. Luo, M. Fan, Z. Xu, and G. Sun, "Byzantine resistant secure blockchained federated learning at the edge," *IEEE Netw.*, vol. 35, no. 4, pp. 295–301, Jul. 2021.
- [16] H. Chai, S. Leng, Y. Chen, and K. Zhang, "A hierarchical blockchain-enabled federated learning algorithm for knowledge sharing in internet of vehicles," *IEEE Trans. Intell. Transp. Syst.*, vol. 22, no. 7, pp. 3975–3986, Jul. 2021.
- [17] Y. Liu, Y. Lan, B. Li, C. Miao, and Z. Tian, "Proof of learning (PoLe): Empowering neural network training with consensus building on blockchains," *Comput. Networks*, vol. 201, p. 108594, Nov. 2021.
- [18] K. Toyoda and A. N. Zhang, "Mechanism design for an incentive-aware blockchain-enabled federated learning platform," in *Proc. 2019 IEEE Int. Conf. Big Data*, Los Angeles, CA, USA, Dec. 2019, pp. 395–403.
- [19] P. Ramanan and K. Nakayama, "BAFFLE: Blockchain based aggregator free federated learning," in *Proc. 2020 IEEE Int. Conf. Blockchain*, Rhodes, GR, Nov. 2020, pp. 72–81.
- [20] X. Qu, S. Wang, Q. Hu, and X. Cheng, "Proof of federated learning: A novel energy-recycling consensus algorithm," *IEEE Trans. Parallel Distrib. Syst.*, vol. 32, no. 8, pp. 2074–2085, Aug. 2021.
- [21] Y. Wang, H. Peng, Z. Su, T. H. Luan, A. Benslimane, and Y. Wu, "A platform-free proof of federated learning consensus mechanism for sustainable blockchains," *IEEE J. Sel. Areas Commun.*, vol. 40, no. 12, pp. 3305–3324, Dec. 2022.
- [22] Y. Liu, Z. Ai, S. Sun, S. Zhang, Z. Liu, and H. Yu, "FedCoin: A peer-to-peer payment system for federated learning," in *Federated Learn.: Privacy Incentive*, Q. Yang, L. Fan, and H. Yu, Eds. Cham, CH: Springer, Nov. 2020, pp. 125–138.
- [23] M. Cao, L. Zhang, and B. Cao, "Toward on-device federated learning: A direct acyclic graph-based blockchain approach," *IEEE Trans. Neural Netw. Learn. Syst.*, vol. 34, no. 4, pp. 2028–2042, Apr. 2023.
- [24] X. Ying, C. Liu, and D. Hu, "GCFL: Blockchain-based efficient federated learning for heterogeneous devices," in *Proc. 28th IEEE Symp. Computers Commun. (ISCC'23)*, Los Alamitos, CA, USA, Jul. 2023, pp. 1033–1038.
- [25] C. Zhang, Y. Xu, X. Wu, E. Wang, H. Jiang, and Y. Zhang, "A semi-asynchronous decentralized federated learning framework via tree-graph blockchain," in *Proc. 2024 IEEE Conf. Comput. Commun. (INFOCOM)*, Vancouver, BC, Canada, May 2024, pp. 1121–1130.
- [26] X. Zhang, Z. Xu, H. Cheng, T. Che, K. Xu, W. Wang, W. Zhao, C. Wang, and Q. Li, "Secure collaborative learning in mining pool via robust and efficient verification," in *Proc. IEEE 43rd Int. Conf. Distrib. Comput. Syst. (ICDCS'23)*, Hong Kong, CN, Jul. 2023, pp. 794–805.
- [27] H. Jia, M. Yaghini, C. A. Choquette-Choo, N. Dullerud, A. Thudi, V. Chandrasekaran, and N. Papernot, "Proof-of-learning: Definitions and practice," in *Proc. 2021 IEEE Symp. Secur. Privacy (SP)*, San Francisco, CA, USA, May 2021, pp. 1039–1056.
- [28] X. Su, M. Larangeira, and K. Tanaka, "Provably secure blockchain protocols from distributed proof-of-deep-learning," in *Proc. 17th Int. Conf. Netw. Syst. Secur.*, Canterbury, UK, Aug. 2023, pp. 114–136.
- [29] C. Chenli, B. Li, and T. Jung, "DLchain: Blockchain with deep learning as proof-of-useful-work," in *Proc. 16th IEEE World Cong. Services (SERVICES'20)*, Honolulu, HI, USA, Sep. 2020, pp. 43–60.
- [30] H. Zhang, J. Wu, X. Lin, A. K. Bashir, and Y. D. Al-Otaibi, "Integrating blockchain and deep learning into extremely resource-constrained IoT: An energy-saving zero-knowledge PoL approach," *IEEE Internet Things J.*, vol. 11, no. 3, pp. 3881–3895, Feb. 2024.
- [31] L. Breiman, "Bagging predictors," *Mach. Learn.*, vol. 24, no. 2, pp. 123–140, Aug. 1996.
- [32] F. Tschorsch and B. Scheuermann, "Bitcoin and beyond: A technical survey on decentralized digital currencies," *IEEE Commun. Surveys Tut.*, vol. 18, no. 3, pp. 2084–2123, 3rd Quart. 2016.

- [33] J. Garay, A. Kiayias, and N. Leonardos, "The bitcoin backbone protocol: Analysis and applications," *J. ACM*, vol. 71, no. 4, pp. 1–49, Aug. 2024.
- [34] L. Deng, "The MNIST database of handwritten digit images for machine learning research [best of the web]," *IEEE Signal Process. Mag.*, vol. 29, no. 6, pp. 141–142, Nov. 2012.
- [35] A. Krizhevsky, "Learning multiple layers of features from tiny images," 2009. [Online]. Available: <https://www.cs.toronto.edu/~kriz/learning-features-2009-TR.pdf>
- [36] Y. Netzer, T. Wang, A. Coates, A. Bissacco, B. Wu, A. Y. Ng *et al.*, "Reading digits in natural images with unsupervised feature learning," presented at the NIPS 2011 Workshop Deep Learn. Unsupervised Feature Learn., Granada, ES, Dec. 2011, pp. 1–9.
- [37] S. Caldas, S. M. K. Duddu, P. Wu, T. Li, J. Konečný, H. B. McMahan, V. Smith, and A. Talwalkar, "LEAF: A benchmark for federated settings," *arXiv preprint arXiv:1812.01097*, Dec. 2019.
- [38] Y. Lecun, L. Bottou, Y. Bengio, and P. Haffner, "Gradient-based learning applied to document recognition," *Proc. IEEE*, vol. 86, no. 11, pp. 2278–2324, Nov. 1998.
- [39] K. He, X. Zhang, S. Ren, and J. Sun, "Deep residual learning for image recognition," in *Proc. 29th IEEE Conf. Comput. Vis. Pattern Recognit. (CVPR'16)*, Las Vegas, NV, USA, Jun. 2016, pp. 770–778.
- [40] G. Huang, Z. Liu, L. V. D. Maaten, and K. Q. Weinberger, "Densely connected convolutional networks," in *Proc. 30th IEEE Conf. Comput. Vis. Pattern Recognit. (CVPR'17)*, Honolulu, HI, USA, Jul. 2017, pp. 2261–2269.
- [41] M. Sandler, A. Howard, M. Zhu, A. Zhmoginov, and L. Chen, "MobileNetV2: Inverted residuals and linear bottlenecks," in *Proc. 31th IEEE Conf. Comput. Vis. Pattern Recognit. (CVPR'18)*, Salt Lake City, UT, USA, Jun. 2018, pp. 4510–4520.
- [42] Q. Li, Y. Diao, Q. Chen, and B. He, "Federated learning on non-IID data silos: An experimental study," in *Proc. IEEE 38th Int. Conf. Data Eng. (ICDE'22)*, Kuala Lumpur, MY, May 2022, pp. 965–978.
- [43] H. Zhu, J. Xu, S. Liu, and Y. Jin, "Federated learning on non-IID data: A survey," *Neurocomputing*, vol. 465, pp. 371–390, Nov. 2021.